

In tetragonal³⁵ complexes the parent octahedral transition (${}^3A_{2g} \rightarrow {}^3T_{2g}$) is split into two transitions, ${}^3B_{1g} \rightarrow {}^3B_{2g}$ and ${}^3B_{1g} \rightarrow {}^3E_g$. The energy of the former tetragonal component is a measure of the in-plane donor strength, whereas the latter component is a function of the axial donor strength. For a series of complexes in which only the weaker axial donors are varied, the energy of the in-plane transition should remain approximately constant while the energy of the axial transition decreases in going to poorer axial donors. For in-plane and axial ligands of comparable donor strength, the separation of the tetragonal levels becomes too small to be observed.

Although the number of nickel(II) bands observed in the solid-state spectra of the halide complexes is too low to permit a detailed analysis, a tentative assignment can be made using this tetragonal crystal field model assuming D_{4h} to be the donor atom symmetry.³⁶ The lowest energy component of ν_1 corresponds to the axial ${}^3B_{1g} \rightarrow {}^3E_g$ transition, and the remaining more intense higher energy component to the in-plane ${}^3B_{1g} \rightarrow {}^3B_{2g}$ transition. The third weaker feature seen in ν_1 for some of these complexes could arise from the ${}^1B_{1g} \rightarrow {}^1A_{1g}$, ${}^1B_{1g}$ transition. The method of calculation outlined by Lever³⁵ yields average values (cm^{-1}) of 305, 390, 530, and 750 for the axial ligand field strength of I^- , Br^- , Cl^- , and H_2O (in $Ni(py_2tn)Cl_2 \cdot 6H_2O$), respectively. These values are only approximate, but they do correspond to values reported for other tetragonal nickel(II) systems and to the order predicted by the spectrochemical series.^{34,35} The average value of

(36) The actual symmetry of the complexes is C_2 or lower depending on the central ring substituents.

the ligand crystal field strength (1300 cm^{-1}) is close to that observed for bipyridyl (1265 cm^{-1}), which is expected because of the similarity of the ligands.

For the complexes containing azide, nitrite, thiocyanate, and imidazole, ν_1 and ν_2 may be assigned to the ${}^3A_{2g} \rightarrow {}^3T_{2g}$ and ${}^3A_{2g} \rightarrow {}^3T_{1g}(F)$ transitions of octahedral nickel(II), and the shoulder observed on ν_1 to the spin-forbidden ${}^3A_{2g} \rightarrow {}^1E_g$ transition. The apparent lack of tetragonal splitting in ν_1 can be ascribed to the smaller difference between the planar and axial ligand field strengths for these derivatives.

Registry No. Potassium phthalimide, 1074-82-4; 1,3-dibromobutane, 107-80-2; 1,3-bis(phthalimidyl)butane, 39489-17-3; hydrazine, 302-01-2; 1,3-diaminobutane, 590-88-5; pyridine-2-carboxaldehyde, 1121-60-4; py_2tn , 39489-18-4; 1,3-diamino-2-propanol, 616-29-5; py_2tnOH , 39489-19-5; $Ni(py_2tnOH)Cl_2$, 39546-56-0; $Ni(py_2tnOH)Br_2$, 39489-13-9; $Ni(py_2tnOH)I_2$, 39489-12-8; $Ni(py_2tnOH)(NO_2)_2$, 39546-55-9; $Ni(py_2tnOH)(N_3)_2$, 39489-11-7; $Ni(py_2tnOH)(NCS)_2$, 39489-10-6; $Ni(py_2tn)Cl_2$, 39489-09-3; $Ni(py_2tn)Br_2$, 39489-08-2; $Ni(py_2tn)I_2$, 39489-07-1; $Ni(py_2tn)(NO_2)_2$, 39489-06-0; $Ni(py_2tn)(N_3)_2$, 39489-05-9; $Ni(py_2tn)(NCS)_2$, 39489-04-8; $Ni(py_2tn)(Im)_2I_2$, 39489-03-7; $Ni(py_2tn)(+tnCH_3)Cl_2$, 39489-02-6; $Ni(py_2tn)(+tnCH_3)(N_3)_2$, 39489-01-5; $Ni(7-CH_3py_2tn)Cl_2$, 39489-00-4; $Ni(7-CH_3py_2tnCH_3)Cl_2$, 39488-99-8.

Acknowledgment. This research was supported by a grant from the Petroleum Research Fund, administered by the American Chemical Society.

Contribution from the Department of Chemistry,
Case Western Reserve University, Cleveland, Ohio 44106

Electronic, Circular Dichroism, and Proton Magnetic Resonance Spectral Studies of the Nickel(II) Complexes of Some Neutral, Tetradentate Schiff Base Ligands Derived from 1,3-Diamines

T. G. CAMPBELL¹ and F. L. URBACH*

Received January 30, 1973

The nickel(II) complexes of the four neutral, tetradentate Schiff base ligands derived from pyridine-2-carboxaldehyde or 2-acetylpyridine and 1,3-diaminopropane or 1,3-diaminobutane were characterized in solution by conductivity measurements and absorption, circular dichroism, and proton magnetic resonance spectroscopy. The complexes $[Ni(\text{ligand})X_n] \cdot nH_2O$, where $X^- = Cl^-, Br^-, I^-$, or NO_2^- , behave as 2:1 electrolytes in aqueous solution and give rise to a common species formulated as $[Ni(\text{ligand})(H_2O)_2]^{2+}$. The azide derivatives are formulated as $[Ni(\text{ligand})(N_3)(H_2O)]^+$ in water and the chloride complexes as $[Ni(\text{ligand})(Cl)(CH_3OH)]^+$ in methanol. In aqueous solution the complex ion $[Ni(\text{ligand})(H_2O)_2]^{2+}$ reacts with additional neutral monodentate donors to yield $[Ni(\text{ligand})(\text{donor})_2]^{2+}$. The solution electronic spectra of the complexes exhibit a pronounced tetragonal splitting in the band attributed to the lowest energy octahedral nickel(II) transition. The circular dichroism spectra of the complexes with Schiff bases derived from (*S*)-(+)-1,3-diaminobutane show features similar to the electronic spectra and are consistent with a tetragonal model. The contact-shifted proton magnetic resonance spectra of the paramagnetic complexes confirm the Schiff base nature and tetradentate coordination of the ligands. The pmr studies indicate a preferred methyl axial conformation for the central chelate ring in the nickel(II) Schiff base complexes derived from 1,3-diaminobutane.

Introduction

In a previous paper² we reported the preparation and solid-state characterization of the nickel(II) complexes with the ligand *N,N'*-bis(2-pyridylmethylene)-1,3-diaminopropane

and several related Schiff bases. This paper describes the studies undertaken to establish the stereochemistry of these complexes in solution.

Experimental Section

The following abbreviations are used for the tetradentate ligands: py_2tn , *N,N'*-bis(2-pyridylmethylene)-1,3-diaminopropane; $py_2(+tn)CH_3$, *N,N'*-bis(2-pyridylmethylene)-(*S*)-(+)-1,3-diaminobutane; $7-CH_3py_2tn$, *N,N'*-bis(7-methyl-2-pyridylmethylene)-1,3-diaminopropane; $7-CH_3py_2tnCH_3$, *N,N'*-bis(7-methyl-2-pyridylmethylene)-1,3-diaminobutane.

(1) National Institutes of Health Predoctoral Fellow; Fellowship 5 F01 GM 39525-02 from the National Institute of General Medical Sciences.

(2) T. G. Campbell and F. L. Urbach, *Inorg. Chem.*, **12**, 1836 (1973).

Syntheses. Preparations for the nickel(II) complexes are described in the previous paper.²

N-Methyl-2-pyridylaldimine, *pyamn*, was prepared by the method of Figgins and Busch³ and was used within 3 days; bp 75° (9.5 mm uncor); lit.³ bp 64° (9 mm).

[*N,N'*-Bis(2-pyridylmethylene)-1,3-diaminopropane]zinc(II) Nitrate, Zn(*pya*₂tn)(NO₃)₂. A solution of 1,3-diaminopropane (1.40 ml, 16.6 mmol) in 50 ml of absolute ethanol was added to pyridine-2-carboxaldehyde (3.17 ml, 33.3 mmol). The resulting yellow solution was cooled to room temperature and then added dropwise to a solution of zinc nitrate (Zn(NO₃)₂·6H₂O, 4.96 g, 16.6 mmol) in 50 ml of absolute ethanol. The solution turned brown, and off-white crystals precipitated on standing. The crystals were filtered, washed with absolute ethanol, and dried *in vacuo*; yield 5.2 g. *Anal.* Calcd for C₁₅H₁₆N₆O₆Zn: C, 40.63; H, 3.55; N, 18.99. Found: C, 40.79; H, 3.65; N, 19.03. (Galbraith Analytical Laboratories, Knoxville, Tenn.).

Physical Measurements. Conductivity measurements were made using an Industrial Instruments Model RC16B2 conductivity bridge. The conductivity cell constant ($\theta = 1.434 \pm 0.007 \text{ cm}^{-1}$) was determined using 0.1000 *M* KCl solutions. Distilled water and absolute methanol used as solvents gave specific conductivities of 1.7×10^{-6} and $1.0 \times 10^{-6} \text{ ohm}^{-1} \text{ cm}^{-1}$, respectively. Molar conductivities were reproducible to $\pm 2 \text{ cm}^2 \text{ ohm}^{-1} \text{ mol}^{-1}$ in the concentration range 8–50 *mM*. Temperature variation was $\pm 0.2^\circ$.

Electronic absorption spectra in solution between 7.5 and 45 kK were obtained at ambient temperatures using Cary Models 14 and 15 recording spectrophotometers. Solutions of Ni(*pya*₂tn)Cl₂·H₂O within the concentration range 8–100 *mM* in water and 16–100 *mM* in methanol showed no deviations from Beer's law in the 9–20-kK region of the spectrum.

Circular dichroism spectra for the *pya*₂(+)*tnCH*₃ complexes in the range 14–40 kK were obtained using a Cary Model 60 recording spectropolarimeter equipped with the Model 6001 circular dichroism accessory. Spectra in the 8.5–14-kK region were obtained with a Shimadzu QV-50 spectrophotometer equipped with a Type VCD-1 circular dichroism attachment.⁴ Solutions of the corresponding *pya*₂tn complexes were used to determine the base line. Measurements of per cent transmittance for both left and right circularly polarized light were made at 10-nm intervals. Calculated $\Delta\epsilon$ values were reproducible to $\pm 2\%$.

Proton magnetic resonance spectra for the nickel(II) complexes were obtained using a Varian HA-100 spectrometer operating in "Mon Lock" mode with a modulation frequency of 30 kHz supplied by an external generator and calibrated using a V-4315 frequency counter. The low signal to noise ratio resulting from the use of 30-kHz modulation was significantly improved through the use of modified compensated driver amplifier circuit, Varian 910884-01.

Signals were recorded without an internal lock by sweeping the magnetic field with the V-3507 slow-sweep unit. Spectra recorded by both increasing and decreasing the field strength were identical. A typical scan of 40 kHz required approximately 15 min with careful adjustment of the slow-sweep unit to minimize magnet drift. Since the resonances showed no tendency to saturate, high power levels were employed to maximize signal size. The temperature of the samples was maintained within $\pm 1^\circ$ using a V-6040 variable-temperature controller, calibrated using ethylene glycol. Resonance positions were calibrated by the modulation side-band method and were reproducible to between ± 0.1 and ± 1.5 ppm, depending on the half-bandwidth of the signal. Spectra recorded in the HR instrument mode were found to give the same results, but with much poorer signal to noise ratios.

The pmr spectra were measured in D₂O solutions containing approximately 14% complex by weight. Several samples with concentrations varying from 10 to 20% by weight showed no changes in resonance positions within experimental error. Tetramethylammonium chloride, TMAC, was employed as an internal reference.

The spectrum of Zn(*pya*₂tn)(NO₃)₂ in D₂O solution containing tetramethylammonium chloride was recorded using normal operating procedures with sodium 3-(trimethylsilyl)-1-propanesulfonate as the standard. The spectrum was assigned by consideration of integrated areas and by comparison to the assignments reported for *pya*₂en.⁵ No attempt was made to analyze the complex patterns found for the pyridine and methylene protons.

(3) P. E. Figgins and D. H. Busch, *J. Phys. Chem.*, **65**, 2236 (1961).

(4) The authors wish to thank Preiser Scientific Co. for the loan of the QV-50 spectrophotometer.

(5) D. A. Durham and F. A. Hart, *J. Inorg. Nucl. Chem.*, **31**, 145 (1969).

Table I. Molar Conductivities of the Nickel(II) Complexes

Complex	Solvent	Concn, mM	Λ_M (25.0°), cm ² ohm ⁻¹ mol ⁻¹	Assigned electrolyte type
Ni(<i>pya</i> ₂ tn)Cl ₂ ·H ₂ O	H ₂ O	16	192 ^a	2:1
	CH ₃ OH	16	88	1:1
Ni(<i>pya</i> ₂ tn)Br ₂	H ₂ O	16	187	2:1
Ni(<i>pya</i> ₂ tn)I ₂	H ₂ O	20	175	2:1
Ni(<i>pya</i> ₂ tn)(NO ₃) ₂	H ₂ O	16	175	2:1
Ni(<i>pya</i> ₂ tn)(N ₃) ₂	H ₂ O	16	111	1:1
Ni(<i>pya</i> ₂ (+) <i>tnCH</i> ₃)Cl ₂ ·2H ₂ O	H ₂ O	16	189 ^a	2:1
	CH ₃ OH	14	85 ^a	1:1
Ni(<i>pya</i> ₂ (+) <i>tnCH</i> ₃)(N ₃) ₂ ·H ₂ O	H ₂ O	16	112	1:1
Ni(7-CH ₃ <i>pya</i> ₂ tn)Cl ₂	H ₂ O	17	189 ^a	2:1
	CH ₃ OH	14	98 ^a	1:1

^a At 25.4°.

Results and Discussion

Conductance. The molar conductivity values and assigned electrolyte types are given in Table I for the complexes in the concentration region employed for spectral studies. The deduction of electrolyte type was made by comparing the observed molar conductivities to values reported for various salts at similar concentrations^{6,7} and for various complex ions.⁸ The complexes formulated as 1:1 electrolytes in *ca.* 16 *mM* solutions gave molar conductivities approaching values typical of 2:1 electrolytes at concentrations near 1 *mM*.

Electronic Spectra. The solution spectra of the nickel(II) complexes in the near-infrared and visible regions consist of two principal bands ν_1 and ν_2 (Table II). These bands are in the spectral region where the first two spin-allowed transitions are expected for octahedral nickel(II) complexes, and display the same weak intensity ($\epsilon \sim 10$). The extra features seen in the low-energy band (ν_1), and the changes in this band accompanying changes in solvent may be interpreted using the tetragonal crystal field model.⁹ The use of the tetragonal model presupposes an essentially planar disposition of the tetradentate ligand around the nickel(II) ion, with the remaining two axial coordination sites in solution occupied by donors of variable strength.

Since the solution spectra of the nickel(II) complexes of *pya*₂tn and *pya*₂(+)*tnCH*₃ are nearly identical, the following discussion applies equally to complexes of both ligands. All of the Ni(*pya*₂tn)X₂ complexes formulated as 2:1 electrolytes (X⁻ = Cl⁻, Br⁻, I⁻, NO₂⁻) yield identical spectra in aqueous solution and the common species is formulated as [Ni(*pya*₂tn)(H₂O)₂]²⁺. The spectrum of this complex ion (Figure 1A) shows a splitting in the low-energy band (ν_1) as a result of the difference in strength between the in-plane nitrogen donors and the weaker axial water donors. The shoulder at 10 kK is assigned to the axial component¹⁰ and the band at 12.5 kK to the in-plane component. The tetragonal splitting for the second octahedral band (ν_2) is expected⁹ to be smaller and is not observed. The remaining weak shoulder at 13.2 kK is assigned to a spin-forbidden transition. The

(6) "The International Critical Tables," Vol. VI, McGraw-Hill, New York, N. Y., 1929; Landolt-Bornstein, "Zahlenwerte und Funktionen," Vol. II, Part 7, 6th ed, Springer-Verlag, Berlin, 1960.

(7) P. A. D. de Maine and P. J. Santiago, *J. Miss. Acad. Sci.*, **8**, 282 (1962).

(8) R. A. Krause and D. H. Busch, *J. Amer. Chem. Soc.*, **82**, 4830 (1960); M. A. Robinson and D. H. Busch, *Inorg. Chem.*, **2**, 1171 (1963); L. V. Interrante, *ibid.*, **7**, 943 (1968); R. D. Feltham and R. G. Hayter, *J. Chem. Soc.*, 4587 (1964).

(9) A. B. P. Lever, *Coord. Chem. Rev.*, **3**, 119 (1968).

(10) The terms "in-plane" and "axial" used to describe transitions or band components of ν_1 refer to the transitions from the ³B_{1g} (*D_{4h}*) ground state to the tetragonal levels ³B_{2g} and ³E_g, respectively.

Table II. Visible and Near-Infrared Electronic Spectral Data

Complex	Solvent	$\bar{\nu}$, kK (ϵ , l. mol ⁻¹ cm ⁻¹)	
		ν_1	ν_2
Ni(py ₂ ,tn)Cl ₂ ·H ₂ O	H ₂ O	10.0 ^a (3), 12.5 (10), 13.2 (9)	18.2 (6)
Ni(py ₂ ,tn)X ₂ , X = Br, I, NO ₂			
Ni(py ₂ ,(+)-tnCH ₃)Cl ₂ ·2H ₂ O			
Ni(7-CH ₃ py ₂ ,tn)Cl ₂	H ₂ O	9.62 (3), 12.6 (7), 13.3 (7)	17.5, ^a 19.2 (6)
Ni(7-CH ₃ py ₂ ,tnCH ₃)Cl ₂			
Ni(py ₂ ,tn)(N ₃) ₂	H ₂ O ^b	10.2 (7), 12.2 (10), 12.6, ^a 13.1 ^a	18.0 (7)
Ni(py ₂ ,(+)-tnCH ₃)(N ₃) ₂ ·H ₂ O			
Ni(py ₂ ,tn)Cl ₂ ·H ₂ O	Aq pyridine ^c	12.2 (12), 12.7 ^a	18.8 (10)
Ni(py ₂ ,tn)I ₂	Aq imidazole ^d	11.9 (12), 12.7 ^a	17.9 (10)
Ni(py ₂ ,(+)-tnCH ₃)Cl ₂ ·2H ₂ O	Aq pyridine ^c	12.2 (10), 12.7 ^a	18.0 (9)
Ni(7-CH ₃ py ₂ ,tn)Cl ₂	Aq pyridine ^c	11.3, ^a 12.3 (9), 12.5 ^a	17.9, ^a 20.0 ^a
Ni(py ₂ ,tn)Cl ₂ ·H ₂ O	CH ₃ OH	9.4 (4), 12.2 (10), 12.6, ^a 13.1 ^a	17.4 (7)
Ni(py ₂ ,(+)-tnCH ₃)Cl ₂ ·2H ₂ O			
Ni(7-CH ₃ py ₂ ,tn)Cl ₂	CH ₃ OH	9.1 (4), 12.3 (7), 12.6 (7), 13.2 (7)	17.2, ^a 18.9 (7)

^a Shoulder. ^b 16 mM. ^c Complex ~0.1 M; 20% pyridine by volume. ^d 16 mM in complex and 75 mM in imidazole.

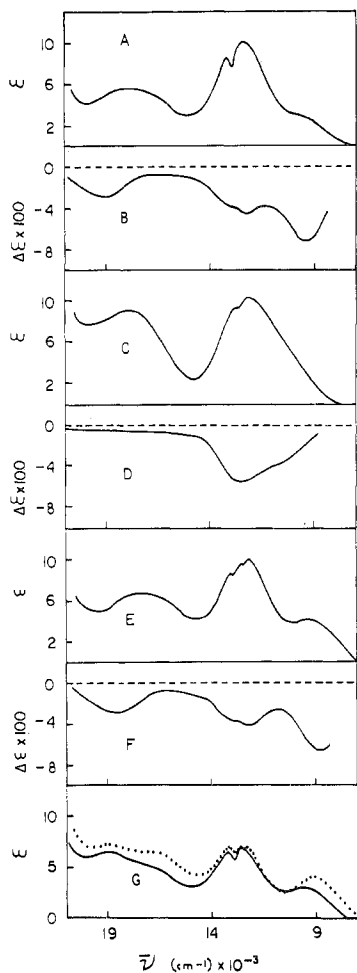


Figure 1. (A) Absorption spectrum of Ni(py₂,(+)-tnCH₃)Cl₂·2H₂O in H₂O. (This spectrum is identical with that of Ni(py₂,tn)Cl₂·H₂O.) (B) Circular dichroism spectrum of Ni(py₂,(+)-tnCH₃)Cl₂·2H₂O in H₂O. (C) Absorption spectrum of Ni(py₂,(+)-tnCH₃)Cl₂·2H₂O in aqueous pyridine (20%). (D) Circular dichroism spectrum of Ni(py₂,(+)-tnCH₃)Cl₂·2H₂O in aqueous pyridine (20%). (E) Absorption spectrum of Ni(py₂,(+)-tnCH₃)Cl₂·2H₂O in methanol. (F) Circular dichroism spectrum of Ni(py₂,(+)-tnCH₃)Cl₂·2H₂O in methanol. (G) Absorption spectra of Ni(7-CH₃py₂,tn)Cl₂ in H₂O (—) and in methanol (---).

spectra of these complexes in aqueous solutions containing imidazole or pyridine (Figure 1C) show no tetragonal splitting in ν_1 , reflecting the comparable donor strengths of these axial nitrogenous bases and the in-plane ligand nitrogen donors. The two principal bands in the spectra obtained in the pres-

ence of strong axial donors are assigned to the two spin-allowed octahedral nickel(II) transitions ${}^3A_{2g} \rightarrow {}^3T_{2g}$ and ${}^3T_{1g} \rightarrow {}^3E_g$ (F), while the weak shoulder is assigned to the spin-forbidden transition ${}^3A_{2g} \rightarrow {}^1E_g$.

The two complexes which are formulated as 1:1 electrolytes, *i.e.*, Ni(py₂,tn)(N₃)₂ in aqueous solution and Ni(py₂,tn)Cl₂·H₂O in methanol, exhibit electronic spectra different from that observed for [Ni(py₂,tn)(H₂O)₂]²⁺. Additional splitting is observed in the in-plane tetragonal component at ~12.5 kK, and the position of the axial tetragonal component of ν_1 reflects the changes in donor strength for a coordinated azide (10.2 kK) or chloride (9.5 kK) (Figure 1E) compared to a coordinated water molecule (10.0 kK).

The spectrum of Ni(7-CH₃py₂,tn)Cl₂ (Figure 1G) is identical with that of Ni(7-CH₃py₂,tnCH₃)Cl₂ and shows more clearly the tetragonal splitting, which is now evident even in the second octahedral band. The axial tetragonal component of ν_1 appears at 9.65 kK, while the in-plane component is assigned to the band at 12.6 kK. The band at 13.3 kK is assigned to the spin-forbidden transition. The tetragonal components of ν_2 appear as a shoulder at 17.5 kK with the maximum at 19.2 kK. In methanol solution (Figure 1G) the 1:1 electrolyte complex shows the axial component of ν_1 at lower energies (9.1 kK) and the split in-plane component centered at 12.5 kK. In aqueous pyridine solution the tetragonal components of ν_1 are closer together, with the axial component evident only as a slight shoulder (11.3 kK) on the in-plane band (12.3 kK).

Circular Dichroism Spectra. An attempt to strengthen the validity of the tetragonal model in assigning the electronic spectra was made by a complementary study of the circular dichroism spectra (Table III). The anticipated advantages of a CD study were that the narrower, signed spectral bands might give increased resolution of the tetragonal components and that the influence of magnetic dipole selection rules might support the band assignments.

The use of magnetic dipole selection rules in assigning CD bands has been discussed by Gillard.¹¹ Only the lowest energy transition for octahedral nickel(II) complexes, ${}^3A_{2g} \rightarrow {}^3T_{2g}$, is magnetic dipole allowed. The higher energy spin-allowed transitions are magnetic dipole forbidden and are expected to give rise to CD bands significantly weaker than the allowed transition. The reduction in symmetry from O_h to D_{4h} accompanying a tetragonal distortion results in a change in the magnetic dipole selection rules. Transitions

(11) R. D. Gillard in "Physical Methods in Advanced Inorganic Chemistry," H. A. O. Hill and P. Day, Eds., Interscience, New York, N. Y., 1968, Chapter 5.

Table III. Circular Dichroism Spectral Data for the $\text{pya}_2(+)\text{tnCH}_3$ Nickel(II) Complexes

Complex	Solvent	$\bar{\nu}$, kK ($\Delta\epsilon \times 10^2$, l. mol ⁻¹ cm ⁻¹)	
		ν_1	ν_2
Ni($\text{pya}_2(+)\text{tnCH}_3$)Cl ₂ ·2H ₂ O	H ₂ O	9.45 (-7.2), 12.3 (-4.5), 12.8 ^a	19.1 (-2.8)
	CH ₃ OH	8.95 (-6.7), 12.2 (-4.2), 12.7 ^a	18.6 (-3.0)
	Aq pyridine ^b	11.0, ^a 12.6 (-5.4)	
Ni($\text{pya}_2(+)\text{tnCH}_3$)(N ₃) ₂ ·H ₂ O	H ₂ O ^c	9.65 (-6.2), 12.2 (-4.2)	19.0 (-2.8)

^a Shoulder. ^b Complex ca. 0.1 M; 20% pyridine by volume. ^c 16 mM.

to the tetragonal components of the first octahedral band (³E_g and ³B_{2g}) remain magnetic dipole allowed, but now transitions to the ³E_g components of the second and third bands also become magnetic dipole allowed. Transitions to the ³A_{2g} tetragonal components of these bands remain magnetic dipole forbidden.

The CD spectrum of Ni($\text{pya}_2(+)\text{tnCH}_3$)Cl₂·2H₂O in water is shown in Figure 1B. The low-energy shoulder on ν_1 at 10 kK in the electronic spectrum, assigned to the axial tetragonal component of the first octahedral band, appears as a distinct CD band at 9.50 kK. The in-plane tetragonal component at 12.5 kK and the spin-forbidden band at 13.3 kK in the electronic spectrum correspond to the CD band at 12.3 kK with a shoulder near 12.8 kK. The CD spectrum shows a band in the region of ν_2 which is comparable in intensity to the components of ν_1 but which is at higher energy than the corresponding band in the electronic spectrum. This 19.1-kK CD band is assigned to the higher energy, magnetic dipole allowed ³E_g tetragonal component of ν_2 .

The CD spectra of the chloride derivative in methanol (Figure 1F) and the azide derivative in water show a similar correspondence to the electronic spectra. Two bands are seen in the region of ν_1 , one near 12.2 kK assigned to the in-plane tetragonal component. The position of the axial component varies according to the strength of the axial donors, moving to slightly higher energy compared to water for the azide, 9.65 kK, and to lower energy for the chloride, 8.95 kK. For each of these complexes a CD band comparable in intensity to the components of ν_1 is seen at energies approximately 1 kK higher than the center of ν_2 in the electronic spectra. These CD bands are assigned to the higher energy magnetic dipole allowed ³E_g tetragonal component of ν_2 .

The CD spectrum in aqueous pyridine (Figure 1D) reflects the change to a more nearly octahedral complex accompanying the presence of the stronger axial pyridine donors. The axial tetragonal component is evident only as a shoulder (11 kK) on the low-energy side of ν_1 (12.6 kK). The CD in the vicinity of ν_2 is negative as found for the other axial donors but is very weak, suggesting that as the nickel(II) ion environment becomes more octahedral, ν_2 becomes magnetic dipole forbidden. For the tris((-)-cyclohexandiamine)nickel(II)¹² and tris((+)-1,2-diaminopropane)nickel(II)¹¹ complex ions, $\Delta\epsilon$ for the lowest energy *O_h* transition was larger than that for the higher energy transitions by a factor of 5 or more. From this observation it was concluded that the *O_h* magnetic dipole selection rules predominated even though the tris(diamine) complexes are formally of *D₃* or *C₃* symmetry. The observed ratio of intensities for ν_1 and ν_2 in the CD spectrum of [Ni($\text{pya}_2(+)\text{tnCH}_3$)(py)₂]²⁺ are consistent with these examples of six-coordinate nickel(II) complexes. The comparable intensities seen for ν_1 and ν_2 in the CD spectra of the $\text{pya}_2(+)\text{tnCH}_3$ complexes in the absence of strong axial donors indicates the applicability of *D_{4h}* selection rules and supports the use of the tetragonal model.

(12) R. S. Treptow, *Inorg. Chem.*, 7, 1229 (1968).

Proton Magnetic Resonance Spectra. The nickel(II) complexes were investigated in solution using proton magnetic resonance spectroscopy in an attempt to confirm the Schiff base nature and tetradentate chelation of the ligands and to support the proposed coordination geometry of the tetradentate ligand deduced from the electronic and circular dichroism spectra. The pmr spectra of the paramagnetic nickel(II) complexes (Table IV) show very large shifts for the ligand protons from the positions seen in the diamagnetic zinc(II) complex.

Since dipolar or pseudocontact shifts have been found to be negligible for nickel(II) complexes,¹³⁻²⁰ the shifts observed for the complexes reported here are considered to be contact shifts as defined by²¹⁻²⁴

$$\delta^c_i(\text{contact shift}) = \delta^p_i(\text{paramagnetic shift}) - \delta^d_i(\text{diamagnetic shift}) \quad (1)$$

Equations 2 and 3 define the contact shift for proton H_i in a paramagnetic complex which obeys the Curie law.²⁴ These

$$\delta^c_i(\text{contact shift}) = -A_i \frac{\gamma e}{\gamma H} g_e \beta_e S(S+1)/3kT \quad (2)$$

$$A_i = \frac{8\pi}{3h} g_e g_H \beta_e \beta_H [\Psi(0)]^2 \quad (3)$$

equations predict that the contact shift for each ligand proton should become zero as the reciprocal of temperature approaches zero and that the contact coupling constant, *A_i*, should be independent of temperature. These predictions can be simultaneously valid only for complexes which obey the Curie law and which undergo no temperature-dependent structural changes or rapid ligand-exchange reactions.²⁵

The pmr spectrum of Ni(pya_2tn)Cl₂ in D₂O, covering 270 ppm, is shown in Figure 2A together with the band assignments. The 3-, 4-, 5-, and 6-H resonances were assigned by comparison to the extensive literature reports for various pyridine derivatives in the presence of nickel(II).^{13,14,17,20,26-29}

- (13) R. E. Cramer and R. S. Drago, *J. Amer. Chem. Soc.*, 92, 66 (1970).
 (14) G. N. La Mar and L. Sacconi, *J. Amer. Chem. Soc.*, 90, 7216 (1968).
 (15) R. J. Fitzgerald and R. S. Drago, *J. Amer. Chem. Soc.*, 90, 2523 (1968).
 (16) J. P. Jesson, *J. Chem. Phys.*, 47, 582 (1967).
 (17) R. H. Holm, G. W. Everett, Jr., and W. DeW. Horrocks, Jr., *J. Amer. Chem. Soc.*, 88, 1071 (1966).
 (18) G. W. Everett, Jr. and R. H. Holm, *J. Amer. Chem. Soc.*, 87, 2117 (1965).
 (19) G. N. La Mar, W. DeW. Horrocks, Jr., and L. C. Allen, *J. Chem. Phys.*, 41, 2126 (1964).
 (20) J. A. Happe and R. L. Ward, *J. Chem. Phys.*, 39, 1211 (1963).
 (21) H. J. Keller and D. E. Schwarzshans, *Angew. Chem., Int. Ed. Engl.*, 9, 196 (1970).
 (22) T. R. Stengle, *Coord. Chem. Rev.*, 2, 349 (1967).
 (23) E. de Boer and H. van Willigan, *Progr. Nucl. Magn. Resonance Spectrosc.*, 2, 111 (1967).
 (24) D. R. Eaton and W. D. Phillips, *Advan. Magn. Resonance*, 1, 103 (1965).
 (25) R. W. Kluiber, R. Kukla, and W. deW. Horrocks, Jr., *Inorg. Chem.*, 9, 1319 (1970).
 (26) J. R. Hutchison, G. N. La Mar, and W. DeW. Horrocks, Jr., *Inorg. Chem.*, 8, 126 (1969).

Table IV. Pmr Data, 25°

Complex	Solvent	Resonance position, δ^{P}_i , ppm from TMAC							
		α -CH	β -CH	3-H	4-H	5-H	6-H	7-H	Other
Zn(py ₂ tn)(NO ₃) ₂	D ₂ O	-1.09 ^a	+0.97 ^a						
NiCl ₂ -pyamn, 1:1	D ₂ O			-48.2	-11.5	-42.8	-152	-236	-113 (N-CH ₃)
NiCl ₂ -tn, ^e 1:2.5	D ₂ O	-147	+12.1						
Ni(py ₂ tn)Cl ₂	D ₂ O	-155	+12.4	-43.1	-10.7	-40.9	-139	-255	
	D ₂ O-pyridine- <i>d</i> ₅ ^b	-155	+12.5	-43.2	-10.7	-41.4	-139	-257	
	CH ₃ OD ^c	-150	+12.1	-41.1	-9.56	-39.5	-135	-249	
Ni(py ₂ (+)-tnCH ₃)Cl ₂	D ₂ O	-107 (ax)	+12.5	-43.6	-10.8	-41.3	-140	-255	<i>d</i>
		-199 (eq)			-11.1				
		-137	+13.3	-54.6	-11.0	-40.2	-150		+17.2 (7-CH ₃)
Ni(7-CH ₃ py ₂ tn)Cl ₂	D ₂ O	-65.5 (ax)	+9.20	-55.4	-10.3	-41.3	-153		+1.02 (α -CH ₃)
Ni(7-CH ₃ py ₂ tnCH ₃)Cl ₂	D ₂ O	-197 (eq)			-10.5	-41.5			+18.3 } (7-CH ₃)
		-248 (eq)							+16.6 } (7-CH ₃)

^a Multiplet center. ^b Pyridine-*d*₅:complex mole ratio 0.95:1. ^c Resonance positions in ppm from CH₃OD. ^d α -CH₃ nearly coincident with TMAC. ^e tn = 1,3-diaminopropane.

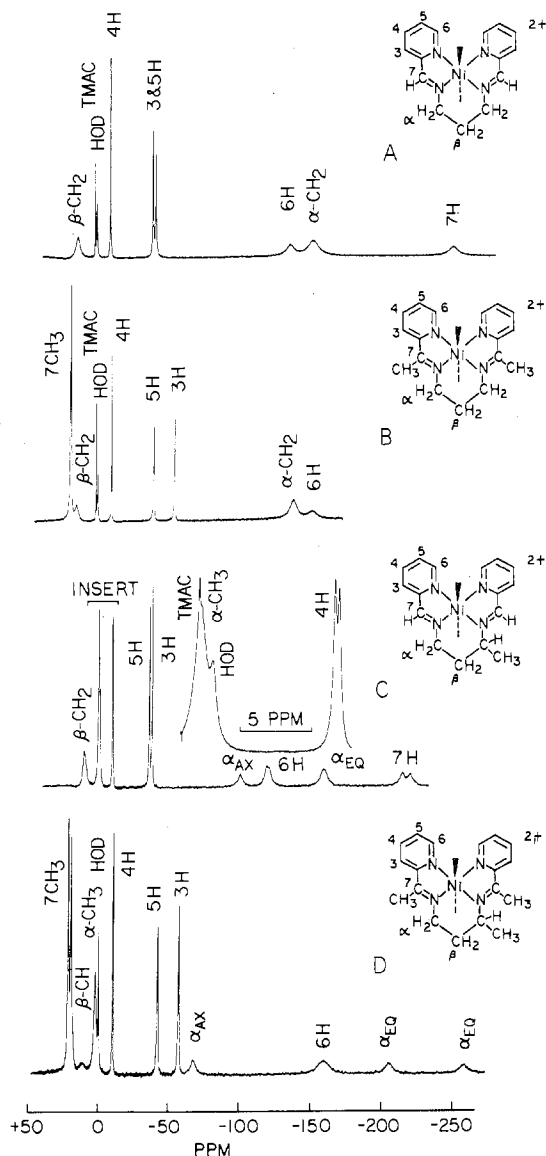


Figure 2. ¹H nmr spectra for the nickel(II) complexes in D₂O at 25°: A, Ni(py₂tn)Cl₂; B, Ni(7-CH₃py₂tn)Cl₂; C, Ni(py₂(+)-tnCH₃)Cl₂ (this spectrum was obtained at 82°); D, Ni(7-CH₃py₂tnCH₃)Cl₂.

The 7-H resonance was assigned by comparison to the spectrum of the 1:1 complex of pyamn with nickel(II) and by the fact that the 7-H signal disappears from the spectra of the complexes prepared from 7-CH₃pya. The α - and β -methylene resonances were assigned from their relative areas and by comparison to the spectra of the nickel(II) complexes of 1,3-diaminopropane and histidine,³⁰ both of which also form six-membered chelate rings.

The single 7-H resonance corresponding in area to two protons confirms the Schiff base nature of the coordinated ligand in solution. The single set of resonances observed for the 3-, 4-, 5-, and 6-H protons indicates that both pyridine moieties are equivalently coordinated, supporting the essentially planar coordination geometry of the tetradentate ligand deduced from the isotropic absorption and circular dichroism spectral studies. The single set of pyridine resonances, however, could also arise from an averaging of the contact coupling constants for protons in nonequivalent pyridine moieties which were rapidly exchanging environments.

Over the temperature range 10–80°, [Ni(py₂tn)(D₂O)₂]²⁺ follows the Curie law as evidenced by linear plots of resonance positions, δ^{P}_i , vs. reciprocal temperature which extrapolate within experimental error to the diamagnetic resonance positions at $T^{-1} = 0$. Although linear Curie law plots for nickel(II) complexes have been taken as evidence for the presence of a single geometric configuration,¹⁴ the temperature dependence of the contact coupling constant^{31,32} is considered to be more sensitive to structural changes. For each proton (except 4-H), the product $|\delta^{\text{P}}_i T|$ which is proportional to the coupling constant A_i , remains constant between 10 and 80° within experimental error, indicating the presence of a single species in solution. A temperature-dependent structural equilibrium between ligand protons in nonequivalent environments could give rise to such temperature-independent contact coupling constants only if the exchange of the protons between environments were rapid and the nonequivalent environments were equally populated at each temperature.

The nmr data for Ni(py₂tn)Cl₂ in methanol-*d*₁ and pyridine-*d*₅-D₂O solutions (Table IV) indicate that no gross structural changes result from a change in axial donor or electrolyte type. The small changes (7 ppm for 7-H, 1 ppm for 4-H) in resonance positions observed in methanol-*d*₁ might

(27) R. W. Kluiber and W. DeW. Horrocks, Jr., *Inorg. Chem.*, **6**, 166 (1967).

(28) M. Wicholas and R. S. Drago, *J. Amer. Chem. Soc.*, **90**, 6946 (1968).

(29) W. DeW. Horrocks, Jr., *Inorg. Chem.*, **9**, 690 (1970).

(30) R. S. Milner and L. Pratt, *Discuss. Faraday Soc.*, **34**, 88 (1962); L. Pratt and B. B. Smith, *Trans. Faraday Soc.*, **65**, 915 (1969).

(31) F. F.-L. Ho and C. N. Reilly, *Anal. Chem.*, **41**, 1835 (1969).

(32) R. M. Golding, P. Healy, P. Newman, E. Sinn, W. C. Tennant, and A. H. White, *J. Chem. Phys.*, **52**, 3105 (1970).

reflect subtle structural changes or could result from the change in internal reference (CH_3OD for TMAC).

Although only small shifts in band positions accompany solvent changes, the effect on bandwidth is pronounced. The half-widths (at half-height) for the resonance signals in methanol- d_1 are uniformly narrower than in D_2O , while the signal half-widths for the pyridine- d_5 - D_2O solutions are broader and increase as the pyridine- d_5 :complex ratio increases. (For a pyridine- d_5 :complex mole ratio of 6.8:1 the downfield resonances can barely be resolved due to the signal broadening.) This line width broadening in the more nearly "octahedral" species containing axial pyridine donors probably results from a decrease in the zero-field splitting (zfs) of the Ni^{2+} ion³³ relative to the tetragonal species with axial water molecules. This decrease in zfs leads to longer electron spin relaxation times and hence to broadened proton resonances.³⁴

Assignments for $\text{Ni}(\text{7-CH}_3\text{pya}_2\text{tn})\text{Cl}_2$ in D_2O (Figure 2B) were made by comparison with the spectrum of $[\text{Ni}(\text{pya}_2\text{tn})(\text{H}_2\text{O})_2]^{2+}$. The resonances for $[\text{Ni}(\text{7-CH}_3\text{pya}_2\text{tn})(\text{D}_2\text{O})_2]^{2+}$ show a uniform decrease in both contact shift and half-width with increased temperature. The contact coupling constants (as $|\delta^p_i T|$) are within experimental error at 25 and 82°.

The spectrum of $\text{Ni}(\text{pya}_2(+)\text{tnCH}_3)\text{Cl}_2$ in D_2O (Figure 2C) is similar to that found for $\text{Ni}(\text{pya}_2\text{tn})\text{Cl}_2$ except that the α -CH protons in $[\text{Ni}(\text{pya}_2(+)\text{tnCH}_3)(\text{D}_2\text{O})_2]^{2+}$ give rise to two signals: one upfield from the α - CH_2 position of $[\text{Ni}(\text{pya}_2\text{tn})(\text{H}_2\text{O})_2]^{2+}$, corresponding in area to one proton, and one downfield signal corresponding to two protons. At higher temperatures, where the contact shifts and half-bandwidths are smaller, the 4- and 7-H resonances are resolved into equal intensity doublets for $[\text{Ni}(\text{pya}_2(+)\text{tnCH}_3)(\text{D}_2\text{O})_2]^{2+}$. Since neither the magnitude of the splitting seen for the 4-H and 7-H doublets nor their relative intensity changes with temperature, the source of the observed splitting must be the result of an inherent difference in coupling constants within the complex caused by the α -methyl substitution.

All of the resonances for $[\text{Ni}(\text{pya}_2(+)\text{tnCH}_3)(\text{D}_2\text{O})_2]^{2+}$ exhibit Curie behavior³⁵ with the exception of the α -CH signals. The deviations of the α -CH resonances from Curie behavior must be the result of a temperature-dependent structural change which gives rise to a change in the contact coupling constant for these protons but does not change A_i for the remaining protons. In a plot of $|\delta^p_i T|$ (which is proportional to A_i) vs. temperature (Figure 3), the β - CH_2 and 3-, 4-, 5-, 6-, and 7-H resonances all yield reasonably straight lines of zero slope as required for constant A_i . The α -CH resonances, however, yield straight lines of opposite slope. The average of the $|\delta^p_i T|$ values for the two α -CH signals at each temperature yields a straight line of zero slope nearly coincident with the line for the α - CH_2 signal in the pya_2tn complex. This type of behavior for the temperature dependence of the coupling constants of α -CH chelate ring protons has been reported for a number of 1,2-diamine and amino acid complexes of nickel(II) by Reilley.^{31,36} Reilley concluded that the structural change responsible for the change in contact coupling constants was a rapid exchange of chelate ring conforma-

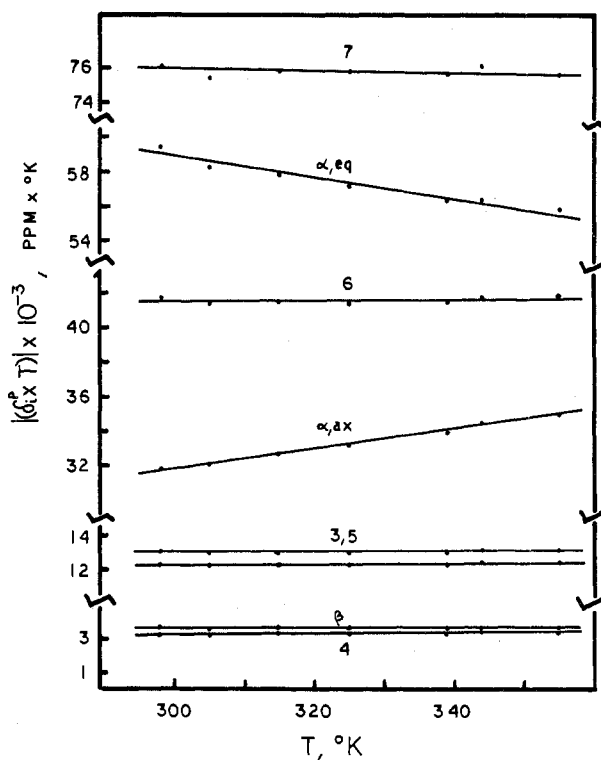
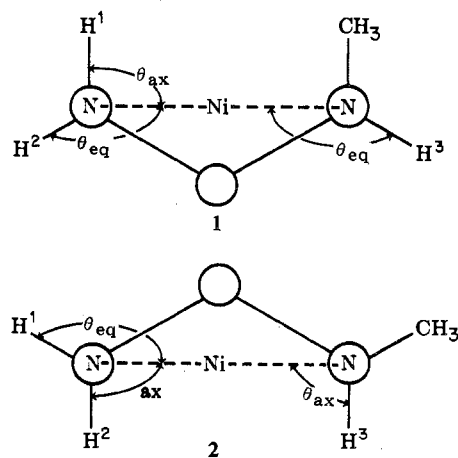


Figure 3. Temperature dependence of contact coupling constants (as $|\delta^p_i T|$) for $\text{Ni}(\text{pya}_2(+)\text{tnCH}_3)\text{Cl}_2$ in D_2O .

tions, with the time-averaged α -CH contact shifts dominated by a structurally favored conformer.

Considerable evidence supports the generalization that the contact coupling constant for a proton in an H-C-N-Ni fragment depends on the dihedral angle between the H-C-N and C-N-Ni planes. For a fragment containing two protons, the proton giving the larger dihedral angle will have the larger coupling constant and hence will experience the larger contact shift.^{15,30,31,36,37} The two idealized conformations of the central chelate ring in $\text{Ni}(\text{pya}_2(+)\text{tnCH}_3)\text{Cl}_2$ are shown by 1 and 2, viewed along the C_α -N axes. For the methyl



equatorial conformer, 2, protons H^2 and H^3 make a smaller dihedral angle (θ_{ax}) than proton H^1 (θ_{eq}). This would cause both H^2 and H^3 to resonate at higher fields than H^1 since both coupling constants are positive. The opposite pattern results in the methyl axial conformer, 1; both H^2 and H^3 , giving the larger dihedral angle (θ_{eq}), will resonate at lower

(33) C. J. Ballhausen, "Introduction to Ligand Field Theory," McGraw-Hill, New York, N. Y., 1962.

(34) W. B. Lewis and L. O. Morgan, *Transition Metal Chem.*, 4, 33 (1968).

(35) G. N. La Mar and G. R. Van Hecke, *J. Amer. Chem. Soc.*, 92, 3021 (1970).

(36) F. F.-L. Ho and C. N. Reilley, *Anal. Chem.*, 42, 600 (1970); F. F.-L. Ho, L. E. Erickson, S. R. Watkins, and C. N. Reilley, *Inorg. Chem.*, 9, 1139 (1970); L. E. Erickson, F. F.-L. Ho, and C. N. Reilley, *ibid.*, 9, 1148 (1970).

(37) T. Yonezawa, I. Morishima, and Y. Ohmori, *J. Amer. Chem. Soc.*, 92, 1267 (1970).

fields than H^1 . The one-proton α -CH resonance is assigned therefore to the axial proton, 1-H, in the α -CH₃ axial conformer, with the downfield two-proton α -CH resonance assigned to the equatorial H^2 and H^3 . Though H^2 and H^3 are nonequivalent as the result of α -methyl substitution, their contact shifts are indistinguishable since they apparently give rise to dihedral angles sufficiently close that the difference in contact coupling constants is less than the bandwidth.

The single α -CH signal observed for the pya_2tn and $7\text{-CH}_3\text{-pya}_2\text{tn}$ complexes can be explained by a rapid conformational exchange of the protons between θ_{ax} and θ_{eq} positions which gives rise to a time-average dihedral angle. For the $\text{pya}_2(+)\text{tnCH}_3$ complex, rapid conformational exchange will also occur, but the existence of separate H_{ax} and H_{eq} resonances indicates that the time-averaged dihedral angles for these protons are dominated by the α -CH₃ axial conformer, 1. The interaction of the α -CH₃ of $\text{pya}_2(+)\text{tnCH}_3$ with the azomethine hydrogen, 7-H, is apparently large enough to give rise to the preferred α -CH₃ axial conformation. The same type of α -CH₃-7-H interaction has been proposed for some tetradentate Schiff base chelate complexes derived from 1,2-diaminopropane, where circular dichroism studies indicate the presence of a preferred α -CH₃ axial conformation for the central 1,2-propane chelate ring.³⁸

The effects of α -CH₃ substitution on the spectrum of the $7\text{-CH}_3\text{pya}_2\text{tn}$ complex is more pronounced than that found for the corresponding pya complexes. The spectrum of $\text{Ni}(7\text{-CH}_3\text{pya}_2\text{tnCH}_3)\text{Cl}_2$ (Figure 2D) shows equal intensity doublets for the 7-CH₃ and 4-, 5-, and 3-H (at 80° only) resonances, and a single resonance for the 6-H. The β -CH₂ resonance appears to be split with one resonance apparent only as a small shoulder on the 7-CH₃ signal seen under conditions of high resolution. The spectrum at 80° gives rise to contact coupling constants (as $|\delta^p/T|$) for all the resonances which are nearly the same within experimental error as those found

at 25°, indicating inherent differences in coupling constants as the source of the band splitting.

The α -CH resonances for the $7\text{-CH}_3\text{pya}_2\text{tnCH}_3$ complex appear as three signals, each corresponding in area to one proton. One resonance appears upfield from the α -CH₂ position in the $7\text{-CH}_3\text{pya}_2\text{tn}$ complex and the other two downfield. The consideration of the dihedral angles made by these protons for both α -CH₃ axial and equatorial leads to the assignments of these protons as axial (upfield) and equatorial (two downfield) with a favored α -CH₃ axial conformation. Framework models indicate severe overlap of the α - and 7-CH_3 groups for an α -CH₃ equatorial conformation. The apparent temperature independence for the α -CH₃ coupling constants indicates this interaction is sufficiently large to prevent an appreciable population of the α -CH₃ equatorial conformation even at 80°. The different coupling constants seen for the two equatorial α -CH protons can result from a difference in their dihedral angles caused by a skewing of the central chelate ring to minimize the α -CH₃-7-CH₃ interaction.

Registry No. $\text{Ni}(\text{pya}_2\text{tn})\text{Cl}_2$, 39489-09-3; $\text{Ni}(\text{pya}_2\text{tn})\text{Br}_2$, 39489-08-2; $\text{Ni}(\text{pya}_2\text{tn})\text{I}_2$, 39489-07-1; $\text{Ni}(\text{pya}_2\text{tn})(\text{NO}_2)_2$, 39489-06-0; $\text{Ni}(\text{pya}_2\text{tn})(\text{N}_3)_2$, 39489-05-9; $\text{Ni}(\text{pya}_2(+)\text{-tnCH}_3)\text{Cl}_2$, 39489-02-6; $\text{Ni}(\text{pya}_2(+)\text{tnCH}_3)(\text{N}_3)_2$, 39489-01-5; $\text{Ni}(7\text{-CH}_3\text{pya}_2\text{tn})\text{Cl}_2$, 39489-00-4; $\text{Ni}(7\text{-CH}_3\text{pya}_2\text{tnCH}_3)\text{Cl}_2$, 39488-99-8; $[\text{Ni}(\text{pya}_2\text{tn})(\text{H}_2\text{O})_2]^{2+}$, 39489-28-6; $[\text{Ni}(\text{pya}_2(+)\text{tnCH}_3)(\text{H}_2\text{O})_2]^{2+}$, 39489-29-7; $[\text{Ni}(7\text{-CH}_3\text{pya}_2\text{tn})(\text{H}_2\text{O})_2]^{2+}$, 39546-58-2; $[\text{Ni}(7\text{-CH}_3\text{pya}_2\text{tnCH}_3)(\text{H}_2\text{O})_2]^{2+}$, 39546-59-3; $[\text{Ni}(\text{pya}_2\text{tn})(\text{N}_3)(\text{H}_2\text{O})]^+$, 39489-30-0; $[\text{Ni}(\text{pya}_2(+)\text{tnCH}_3)(\text{N}_3)(\text{H}_2\text{O})]^+$, 39489-31-1; $[\text{Ni}(\text{pya}_2\text{tn})(\text{py})_2]^{2+}$, 39489-32-2; $[\text{Ni}(\text{pya}_2\text{tn})(\text{imd})_2]^{2+}$, 39489-33-3; $[\text{Ni}(\text{pya}_2(+)\text{tnCH}_3)(\text{py})_2]^{2+}$, 39489-34-4; $[\text{Ni}(7\text{-CH}_3\text{pya}_2\text{tn})(\text{py})_2]^{2+}$, 39489-35-5; $[\text{Ni}(\text{pya}_2\text{tn})(\text{Cl})(\text{MeOH})]^+$, 39489-36-6; $[\text{Ni}(\text{pya}_2(+)\text{tnCH}_3)(\text{Cl})(\text{MeOH})]^+$, 39489-37-7; $[\text{Ni}(7\text{-CH}_3\text{pya}_2\text{tn})(\text{Cl})(\text{MeOH})]^+$, 39489-14-0; $\text{Zn}(\text{pya}_2\text{tn})(\text{NO}_3)_2$, 39489-15-1; $\text{NiCl}_2(\text{pyamn})$, 39489-16-2.

Acknowledgment. This research was supported by a grant from the Petroleum Research Fund, administered by the American Chemical Society.

(38) R. S. Downing and F. L. Urbach, *J. Amer. Chem. Soc.*, **91**, 5977 (1969); **92**, 5861 (1970); R. L. Farmer and F. L. Urbach, *Inorg. Chem.*, **9**, 2562 (1970).